http://www.jourmag.org/index.php/jma

Journal of Magnetism and Its Applications

Received January 28th 2021 received in revised March 30th 2021 accepted April 14th 2021

Research articles

# Detail Synthesis Route of Free-Standing Antiferromagnetic $La_2CuO_4$ Nanoparticles via Sol-gel Method

**Suci Winarsih[1]*, Trisna Maulana[1], Budhy Kurniawan[2]**

[1]Department of Physics, Faculty of Mathematics and Natural Sciences, Universitas Padjadjaran, Raya Bandung-Sumedang St. Km 21, Jatinangor, Sumedang, 45363, Indonesia
[2]Department of Physics, Faculty of Mathematics and Natural Sciences, Universitas Indonesia, Depok 16424, Indonesia

**Article info**

**Keywords:**
Nanoparticles
Sol-gel
Synthesis route
Free-standing antiferromagnetic
$La_2CuO_4$

**Abstract**

We report the detailed synthesis route of free-standing antiferromagnetic $La_2CuO_4$ nanoparticles by the sol-gel method. The precursors were needed to be dissolved in acid solution and continued with heating treatment to make a gel. Some catalyst was needed to control and stabilized the transformation from the solution to gel. Some heating treatments were also conducted to remove the organic component and for the nucleation process to obtain the single-phase sample. Although the sol-gel method required some additional precursors such as acid and catalyst, it has some advantages. It needed a relatively low sintering temperature and short sintering time compare to those at the solid-state reaction. Interestingly, this method can produce a sample with a good distribution of the particle size.

## 1. Introduction

Nano-sized effects have attracted great attention recently since it leads to the alter of physical and magnetic properties of a material. One of the interesting phenomena is the appearance of magnetism in nano-system such as nanogold and nano-CuO [1–5]. Clear evidence of magnetism was observed in gold nanoparticles encapsulated by butanethiol with Au-cluster size at 2.2 nm by muon-spin relaxation ($\mu$SR) [2]. From zero-field, ZF-$\mu$SR time spectra, fast spin relaxation was observed with decreasing temperature indicating the slowing down of electronic magnetic moment fluctuation [2]. The existence of a fluctuating electronic magnetic moment was also confirmed from the longitudinal field, LF-$\mu$SR, in which the slowly relaxation behavior still survives by applying a field of 2 kG [2]. That study could not distinguish whether the magnetic moment is located at the encapsulated molecule or inside the gold nanoparticles. In the case of an antiferromagnetic, CuO, hysteresis loop was also observed when the particle size of about 6.6 nm at 10 K indicating the presence of magnetism [6]. Furthermore, the uncompensated spins at the surface of nanoparticles were proposed to explain the reason behind the appearance of magnetism in CuO nanoparticles.

The suggestion about uncompensated spins at the surface was proposed leading to magnetism in other antiferromagnetic systems such as $La_2CuO_4$. The ferromagnetic component was observed in $La_2CuO_4$ at 20 K until 350 K when its particle size was reduced to 1.53 μm [7]. Both CuO nanoparticles and $La_2CuO_4$ microparticles were not encapsulated by other molecules, but the explanation on these systems is limited to the role of the surface effect only. In the nano-sized effects, there is one more important role. That is the quantum size effect (QSE) which was predicted by Kubo in 1962 [8]. Kubo determined the average of electron level spacing, $\delta$, to be inversely proportional to the density of states, $D(\varepsilon_F)$, at the Fermi energy, $\varepsilon_F$[8]. The physical properties of metallic nanoparticles would significantly differ from the bulk because the energy level of conduction electrons is predicted to become discrete [8, 9], as shown in Eq. 1:

$$\delta = \frac{1}{D(\varepsilon_F)} = \frac{2\pi^2\hbar^2}{m^*(3\pi^2 n)^{\frac{1}{3}}V} \quad (1)$$

where $\hbar$ is Plank's constant, $m^*$ is the effective mass of an electron, $n$ is the electron density, and $V$ is the average volume of the nanoparticles. This prediction is based on the consideration that the electronic state is redistributed near $\varepsilon_F$ when the particle size of a system is reduced down to nanometer size [8, 9]. Even though this theory is believed to happen in nanoparticles, the identification of QSE is still difficult to be observed. This is because when the particle size is reduced to be in nanometer-size, the surface effect will be dominant which also shows the deviation of the physical properties of nanoparticles from the bulk properties [9]. Therefore, it is a challenging part to clarify whether the change of the properties of a system is due to QSE or surface effect.

Among the systems mentioned above, we aim to investigate nano-sized effects in $La_2CuO_4$. The problem that we need to tackle in this system is how to control its particle size within nanometer-size. Some synthesis parameters are needed to be considered to make a single phase of $La_2CuO_4$ nanoparticles. Since the detailed and systematic synthesis route has not been reported yet, we report our detailed synthesis route to produce $La_2CuO_4$ nanoparticles.

## 2. Experimental Methods

The samples were prepared by using a chemical reaction method which is believed to be one of the best methods to produce nanoparticles [10]. Chemical reaction method is a bottom-up method which means spontaneous self-assembly from the atomic level to the nano-scale level. There are some techniques in the chemical reaction method, such as chemical vapor deposition and sol-gel. We chose sol-gel in this study because a sample with a more homogeneous distribution of the particle size could be obtained through this method [11]. Besides that, it needs a relatively low heating treatment.

$La_2O_3$ (Merck, 99.5%) and CuO (Merck, 99.5%) were used as precursors or starting materials. Nitric acid solution (Merck, 69%) was used to dissolve $La_2O_3$ and CuO to make them become $La(NO_3)_3.6H_2O$ and $Cu(NO_3)_2$, respectively. Citric acid monohydrate, $C_6H_8O_7.H_2O$ (Merck, 99.5%) is a weak acid that was used as a chelating agent to control the transformation from solution to be gel so that the uniform gel can be

*Corresponding author
Email: suci.winarsih@unpad.ac.id

DOI: 10.53533/JMA.v1i1.3

achieved. Ethylene glycol, ($C_2H_6O_2$, Merck 99.5%) was used as a stabilizing agent in the sol-gel process. Besides that, citric acid monohydrate and ethylene glycol lead to fasten the bonding reaction among $La^{3+}$, $Cu^{2+}$, and $O^{2-}$. The ratio of CA and EG was 3:2. The role of CA as chelating agent and to fasten the bonding reaction will be active at a certain pH value. The dissociation reactions of CA are shown as Eq. 2 until Eq. 7 [12]. Ammonia solution (Merck, 25%) was used to adjust the pH of the solution.

$$H_3Cit \leftrightarrow H_2Cit^- + H^+ \ (K_{\alpha1} = 7.4 \times 10^{-4}) \quad (2)$$

$$H_2Cit^- \leftrightarrow HCit^{2-} + H^+ \ (K_{\alpha2} = 1.7 \times 10^{-5}) \quad (3)$$

$$HCit^{2-} \leftrightarrow Cit^{3-} + H^+ \ (K_{\alpha3} = 4.0 \times 10^{-7}) \quad (4)$$

$K_{\alpha1}$, $K_{\alpha2}$, $K_{\alpha3}$ are the dissociation constants as described below which are affected by the pH of the solution.

$$K_{\alpha1} = \frac{[H_2Cit^-][H^+]}{[H_3Cit]} \quad (5)$$

$$K_{\alpha2} = \frac{[HCit^{2-}][H^+]}{[H_2Cit^-]} \quad (6)$$

$$K_{\alpha3} = \frac{[Cit^{3-}][H^+]}{[HCit^{2-}]} \quad (7)$$

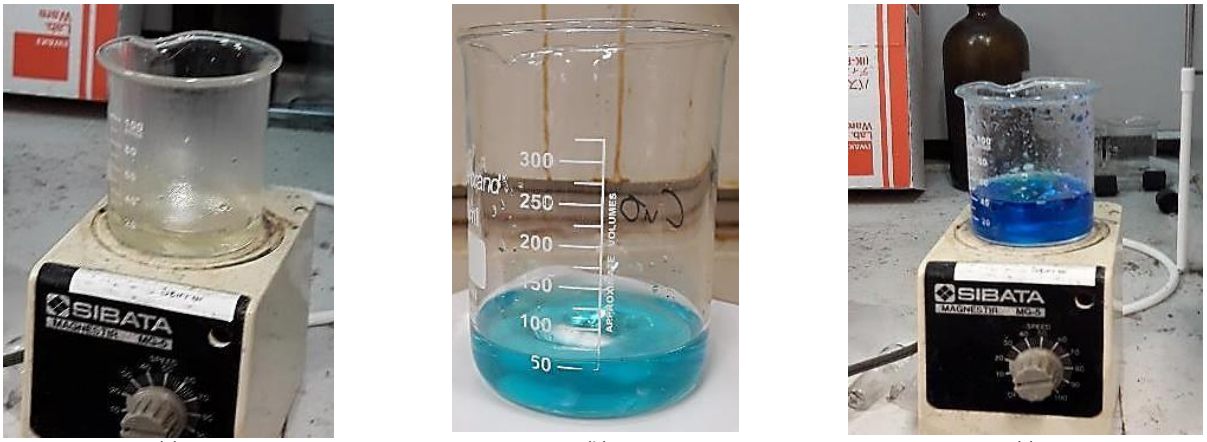
The detailed synthesis route and the sample condition in each step are explained in the next section. X-ray diffraction (XRD) measurement with Cu-Kα radiation at room temperature was performed at the Department of Engineering and Applied Sciences, Sophia University, to check the purity of the samples. The XRD pattern was refined by the Rietveld analysis by using General Structure and Analysis Software (GSAS-II).

## 3. Results and Discussion

As the first step, we need to pre-fire the $La_2O_3$ at 700 °C for two hours since it is sensitive to the air and water. After that, measure the weight of $La_2O_3$ and CuO based on the stoichiometric calculation. Then, dissolved each precursors in the nitric acid solution until a transparent solution was achieved as shown in Fig. 1a and b. After that, mix all of them, then add citric acid monohydrate and ethylene glycol to the solution. The stirring process was done until the transparent solution was achieved, as shown in Fig. 1c. At this stage, the pH of the solution is about 2, which indicates that the citric acid exists as $H_3Cit$ and $H_2Cit^-$. It will be dissociated to be $HCit^{2-}$ and $Cit^{3-}$ when we increase the pH of the solution by adding ammonia solution. We have to add ammonia solution little by little since the temperature of the solution will be automatically increased due to the presence of the ammonia solution. Keep adding the ammonia solution to increase the pH value of the solution. After some trial and error, we got that a pH of 7 is the best condition to make a single phase of $La_2CuO_4$ nanoparticles. Figure 2 shows the solution after achieving a pH of 7.

The next step is to make the solution become gel by setting the temperature of the magnetic stirrer to be around 80 °C and keeping stirring the solution. The gel, as shown in Fig. 3 will be obtained at this stage. Heat the gel at 150 °C to remove all water components from the solution until the dried blue gel was formed, as depicted in Fig. 4. Then, heat it at 300 °C for 3 hours to remove all organic components. This is the so-called calcination process. There was a volume expansion of the sample forming the sponge-like product, as shown in Fig. 5. Grind the sponge-like product to be in a powder form as shown in Fig. 6. Furthermore, the sintering process of the powder for the nucleation process so that the phase of $La_2CuO_4$ will be formed. The minimum sintering condition to make a single phase of $La_2CuO_4$ is 600 °C for 45 minutes [13]. It is lower than that of the solid-state reaction which needs the sintering temperature of above 1000 °C for around 16 hours. After the sintering process, grind the sample to make fine particles. The final product is powder, as depicted in Fig. 7. The heating condition of pre-fire process, calcination, and sintering are shown in Figure 8a, b, and c, respectively.

Figure 9 shows the XRD pattern of the $La_2CuO_4$ nanoparticles. The sample is a single-phase with no impurity phase detected. It means the synthesis route and synthesis parameters used here are in good condition to make $La_2CuO_4$ nanoparticles. Rietveld refinement results have been shown in our former paper showing that the system has orthorhombic crystal structure with *Bmab* space group which is as same as those observed in the bulk case [13]. The particle size of the sample is determined by using TEM showing that the higher sintering temperature and the longer sintering time, the bigger particle size was obtained [13, 14].




(a) (b) (c)

**Fig. 1.** The photograph of (a) $La(NO_3)_3.6H_2O$ solution (b) $Cu(NO_3)_2$ solution (c) Homogeneous solution of $La(NO_3)_3.6H_2O$, $Cu(NO_3)_2$, citric acid, and ethylene glycol.

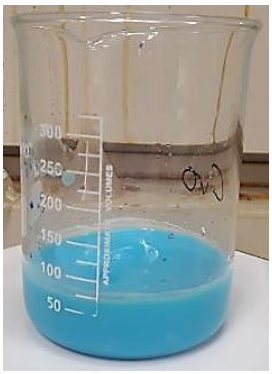


**Fig. 2**. Homogeneous solution after adding ammonia to achieve pH of 7.

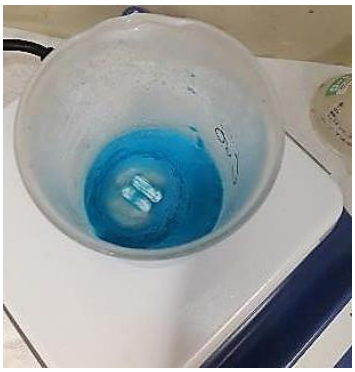


**Fig. 3**. The gel after heating the solution at 80 °C.

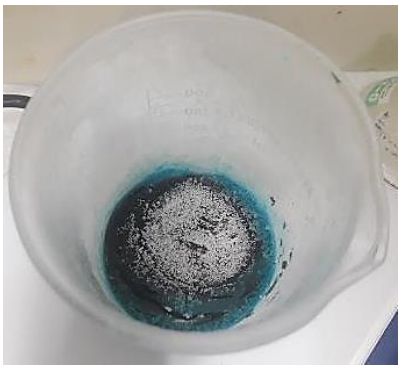


**Fig. 4**. The dried blue gel after removing all water components from the solution.



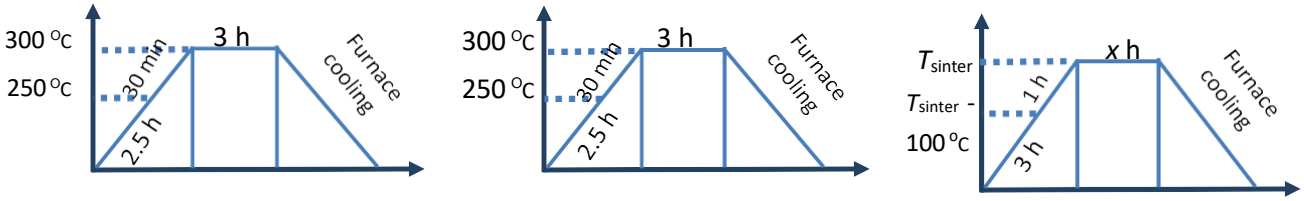
**Fig. 5.** The sponge-like product after the calcination process.



**Fig. 6.** Sample condition after grinding the sponge-like product.



**Fig. 7.** The final product of $La_2CuO_4$ nanoparticles.




(a) (b) (c)

**Fig. 8**. Heating condition of (a) pre-fire process of $La_2O_3$ (b) calcination process (c) sintering process

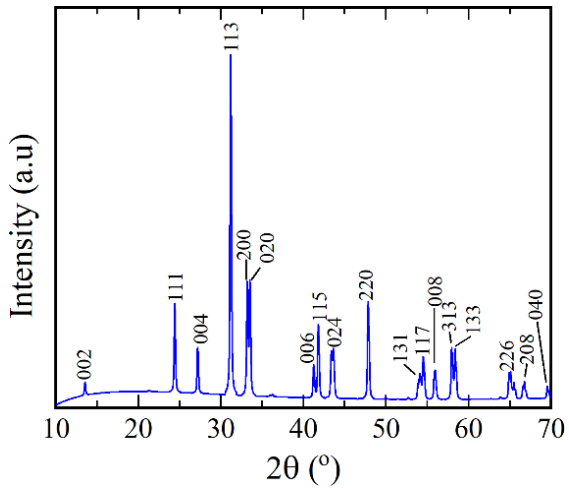



**Fig. 9.** XRD pattern of $La_2CuO_4$ nanoparticles prepared by sol-gel method.

## 4. Conclusions

The preparation of $La_2CuO_4$ nanoparticles was successfully conducted by using the sol-gel method. Some synthesis parameters were needed to be controlled, such as the stoichiometric mass of each precursor, the pH of the solution, the mass ratio between catalysts, sintering time, and sintering temperature. In this work, the $La_2CuO_4$ exhibited a single-phase without impurity phase in nanometric size.

## Acknowledgements

The Post-Doctoral Research Grant supported this work under contract number 3570/UN6.3.3/LT/2020. Authors would like to thank Dr. Isao Watanabe (RIKEN) and Prof. Tadashi Adachi (Sophia University) for their technical support in the X-ray diffraction measurements.

## References

[1] G. L. Nealon, B. Donnio, R. Greget, J. P. Kappler, E. Terazzi, and J. L. Gallani, "Magnetism in gold nanoparticles," *Nanoscale*, vol. 4, no. 17, pp. 5244–5258, 2012, doi: 10.1039/c2nr30640a.

[2] M. H. Dehn *et al.*, "Nature of magnetism in thiol-capped gold nanoparticles investigated with Muon spin rotation," *Appl. Phys. Lett.*, vol. 112, no. 5, 2018, doi: 10.1063/1.5017768.

[3] X. G. Zheng, T. Mori, K. Nishiyama, W. Higemoto, and C. N. Xu, "Dramatic suppression of antiferromagnetic coupling in nanoparticle CuO," *Solid State Commun.*, vol. 132, pp. 493–496, 2004, doi: 10.1016/j.ssc.2004.06.037.

[4] X. G. Zheng *et al.*, "Finite-size effect on Néel temperature in antiferromagnetic nanoparticles," *Phys. Rev. B - Condens. Matter Mater. Phys.*, vol. 72, no. 014464, pp. 1–8, 2005, doi: 10.1103/PhysRevB.72.014464.

[5] a. Punnoose, H. Magnone, M. S. Seehra, and J. Bonevich, "Bulk to nanoscale magnetism and exchange bias in CuO nanoparticles," *Phys. Rev. B - Condens. Matter Mater. Phys.*, vol. 64, no. 174420, pp. 1–8, 2001, doi: 10.1103/PhysRevB.64.174420.

[6] M. S. Seehra and A. Punnoose, "Particle size dependence of exchange-bias and coercivity in CuO nanoparticles," *Solid State Commun.*, vol. 128, pp. 299–302, 2003, doi: 10.1016/j.ssc.2003.08.029.

[7] R. V. Yusupov, V. V. Kabanov, D. Mihailovic, K. Conder, K. A. Müller, and H. Keller, "Spontaneous ferromagnetic spin ordering at the surface of La2 Cu O4," *Phys. Rev. B*, vol. 76, p. 024428, 2007, doi: 10.1103/PhysRevB.76.024428.

[8] R. Kubo, "Electronic Properties of Metallic Fine Particles. I," *J. Phys. Soc. Japan*, vol. 17, no. 6, pp. 975–986, 1962, doi: 10.1143/JPSJ.17.975.

[9] S. Bose and P. Ayyub, "A review of finite size effects in quasi-zero dimensional superconductors," *Reports Prog. Phys.*, vol. 77, p. 116503, 2014, doi: 10.1088/0034-4885/77/11/116503.

[10] A. G. Kolhatkar, A. C. Jamison, D. Litvinov, R. C. Willson, and T. R. Lee, "Tuning the Magnetic Properties of Nanoparticles," *Int. J. Mol. Sci.*, vol. 14, pp. 15977–16009, 2013, doi: 10.3390/ijms140815977.

[11] A. Gaur and G. . D. Varma, "Sintering temperature effect on electrical transport and magnetoresistance of nanophasic $La_{0.7}Sr_{0.3}MnO_3$," *J. Phys. Condens. Matter*, vol. 18, pp. 8837–8846, 2006, doi: 10.1088/0953-8984/18/39/014.

[12] G. Xu, H. Ma, M. Zhong, J. Zhou, Y. Yue, and Z. He, "Influence of pH on characteristics of $BaFe_{12}O_{19}$ powder prepared by sol-gel auto-combustion," *J. Magn. Magn. Mater.*, vol. 301, no. 2, pp. 383–388, 2006, doi: 10.1016/j.jmmm.2005.07.014.

[13] S. Winarsih, F. Budiman, H. Tanaka, T. Adachi, and I. Watanabe, "Growth of Free-Standing $La_{2-x}Sr_xCuO_4$ Nanoparticles," *Mater. Sci. Forum*, vol. 966, pp. 357–362, 2019, doi: 10.4028/www.scientific.net/MSF.966.357.

[14] S. Winarsih, F. Budiman, H. Tanaka, and T. Adachi, "Variable Range Hopping Resistivity in $La_{2-x}Sr_xCuO_4$ Nanoparticles Evaluated by Four Point Probe Method," *Key Eng. Mater.*, vol. 860, pp. 142–147, 2020.